

## Qualitative and quantitative interdependence of physical and mechanical properties of stir-casted hybrid aluminum composites

D. Kumar  , S. Singh , S. Angra

National Institute of Technology Kurukshetra, Haryana, India

✉ [dinesh\\_61900120@nitkkr.ac.in](mailto:dinesh_61900120@nitkkr.ac.in)

**Abstract.** Aluminum alloys are lightweight, castable, machinable, and have good mechanical and physical properties. Aluminum alloys are used in aerospace, automotive, defense, and structural sectors because of their promising qualities. This work examined how stirring speed, preheating temperature, and particle size affect the mechanical characteristics of stir-cast hybrid aluminum nanocomposites supplemented with GNPs and CeO<sub>2</sub> at 0–3 wt. %. The microstructural investigation was done using SEM. EDAX confirmed components in nanocomposite samples. Increased reinforcing percentage improved physical and mechanical properties. The (3 % GNPs and 3 % CeO<sub>2</sub>) hybrid nanocomposites have 1.06 % porosity. The highest hardness, tensile strength, and yield strength were 104.3, 347.01, and 215.13 MPa. SEM micrographs indicated that hybrid composite samples had a more uniform distribution of reinforcements and defects-free morphology.

**Keywords:** Al-6061; nanocomposite; porosity; density; mechanical properties; microstructure

**Citation:** Kumar D, Singh S, Angra S. Qualitative and quantitative interdependence of physical and mechanical properties of stir-casted hybrid aluminum composites. *Materials Physics and Mechanics*. 2023;51(6): 14-23. DOI: 10.18149/MPM.5162023\_2.

### Introduction

The aerospace and automotive sectors, in particular, have expanded their need for sophisticated materials in recent years. In this case, you need a specially formulated combination of materials exhibiting novel and advanced characteristics. [1]. Advanced composite materials can satisfy these requirements. Currently, hybrid composites are being replaced by traditional composites. Hybrid composites have considerable potential in engineering applications owing to their enhanced reliability and performance [2]. The combination of two or more different constituents has distinct physical and chemical characteristics at the microscopic level and possesses better characteristics than the base material, which is termed a hybrid composite material. The hybrid composite has excellent strength-to-weight ratio, stiffness, wear resistance, and corrosion resistance [3–5]. As we are very much aware of the fact that the accessibility of aluminum in Earth's crust is abundant, it is also the second prime metal in the core. Since 1990, aluminum and alloys have been traditionally employed in all engineering sectors, including aerospace, marine, automotive, and structural sectors. Metal matrix composites (MMC) are also made from aluminum by adding very small quantities of reinforcement [6]. Aluminum or aluminum alloys are combined with two or more reinforcing particulates in varying ratios to create hybrid aluminum metal matrix composites (HAMMC). If the reinforcements are nanoparticles, they are termed as nanocomposites. Stir-Cast Hybrid aluminum nanocomposites (HAIMNCs) are popular in various industries because of their enhanced customized mechanical and tribological properties. HAIMNCs also provide a

versatile, attractive, and technological platform for value-added applications such as lithium-ion batteries, superconductors, lightweight structures, and photovoltaic cells [7]. William Hume-Rothery, a metallurgist scientist, described the solubility limits of elements in metals. The enhancement of the characteristics of hybrid nanocomposite materials is greatly dependent on the selection of reinforcements and their distribution throughout the matrix material [8]. A wide range of ceramic and non-ceramic nano-particulates is available for use as reinforcements. Carbon nanotubes, alumina, titanium boride, and silicon carbide have been used as reinforcements [9]. The next most significant factor is the selection of suitable fabrication techniques. The inherent process capability and process-oriented defects are the limitations of traditional casting methods. The overall quality of the fabricated material is also affected by these traditional casting processes. Shrinkage, blow-holes, and dendritic structures are casting defects that affect the mechanical properties of the casted components [10]. To avoid such defects and problems during casting, advanced casting techniques can be used, such as stir casting, friction-stir processing, spray decomposition, and powder metallurgy. The stir casting technique is highly effective in achieving uniform dispersion and strong bonding of reinforcement particles [11]. In this study, nano-powder of graphene and ceria were used as reinforcements owing to their high melting temperatures and low densities, respectively. nanoparticles were also found to enhance the characteristics of the hybrid nanocomposite material. Al-6061 is used as a matrix material because it is lightweight, low-density, has a low melting point, and is applicable in tripartite and quadruple engineering applications. In the course of this investigation, measurements were taken to determine density, porosity, hardness, and tensile strength. The microstructural behavior was also studied to validate the enhancement of the aforementioned properties.

## Materials

**Matrix material.** The matrix used was Al-6061 alloy, and with purity of 98.0 %. A spectrophotometer was used in order to discover the precise chemical components of the Al-6061 alloy, and the alloy contained the following elements and percentages: Si (0.51 %), Fe (0.257 %), Cu (0.219 %), Mn (0.043 %), Zn (0.094 %), Mg (0.797 %), Ni (0.001 %), Cr (0.157 %), Ti (0.027 %), and Al (balance).

**Reinforcement materials.** GNPs (graphene nanoplatelets) and CeO<sub>2</sub> (cerium oxide/ceria). The purity of the CeO<sub>2</sub> powder was 99.5% and the mean particle size was 3-6 nm. The melting temperature of CeO<sub>2</sub> was 3670 °C, and its density was 7.2 g/cm<sup>3</sup>. The purity of GNPs was 99.9 % and the mean particle size was 24-28 nm. The melting temperature of GNPs was 2400 °C, and their density was 2.3 g/cm<sup>3</sup>. The nano-reinforcement particulates were in the range 0–3 wt. % to prepare the test specimens.

## Fabrication method

**Stir-casting procedure.** Hybrid aluminum composite specimens were fabricated using a stir-casting approach, as outlined in the flow diagram (Fig. 1). The electric furnace of the stir-casting machine was superheated at 800 °C and then AA-6061 was added to the electric furnace. Next, graphene and cerium oxide nanoparticles wrapped in aluminum foil were added to the electric furnace. The nano-reinforcements were already preheated at 300 °C for half an hour. This preheating operation was performed to limit the amount of moisture and absorbed gases in the reinforcements, as well as to minimize the temperature differential caused by the addition of particles to the molten metal after it had already been heated. It also reduces the temperature difference of the molten metal after the addition of particulates.

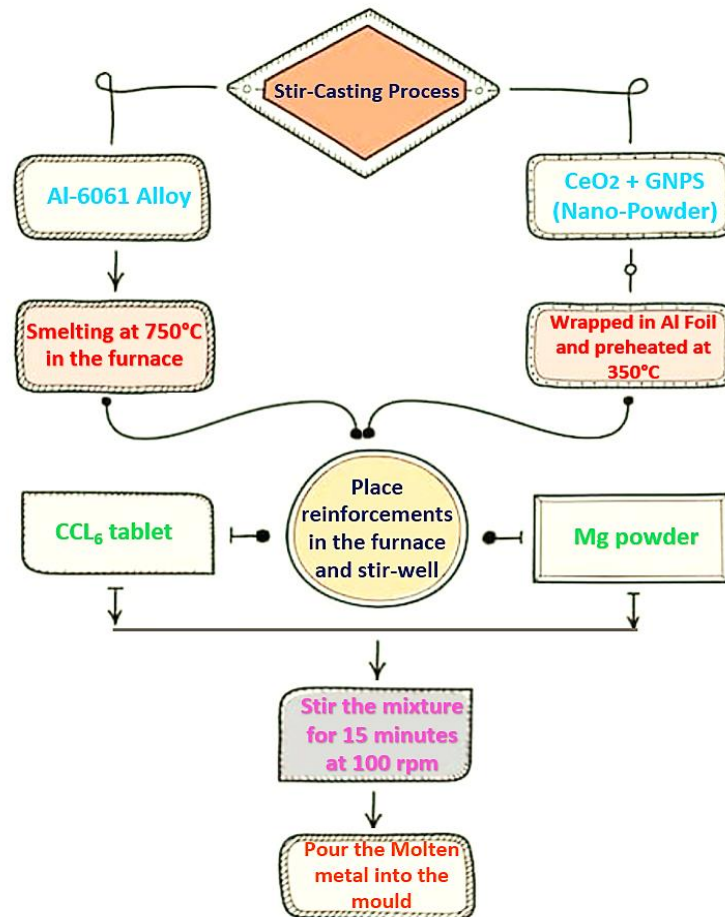


**Fig. 1.** Flow diagram stir casting methods for fabrication of HAIMNCs

Hexachloroethane ( $\text{CCl}_6$ ) tablets were used to degases the molten metal. A temperature of  $750^\circ\text{C}$  was maintained, with adequate viscosity. An appropriate vortex was created using a diamond-coated impeller by stirring at  $350\text{ rpm}$  for 15 minutes. The high stirring speed created a powerful vortex in molten metal, which mixed the nano-reinforcement particles uniformly. This was performed to ensure that the nano-reinforcements were mixed evenly in the base material, which is essential for achieving the desired properties of the produced composites. The addition of 2 % of magnesium was performed to enhance the wettability of the reinforcement particulates. A stirring speed of  $100\text{ rpm}$  was maintained for the next 15 min, followed by a decrease to  $80\text{ rpm}$  for the next 5 min to ensure uniform mixing of the particulates. In the end, the liquid metal was poured into the mould, and then it was left to cool and harden at normal temperature. Four specimens with different compositions were prepared by the stir-casting method, as listed in Table 1.

**Table 1.** Fabricated sample's nomenclature

Sample	Nomenclature	Composition
1	HAIMNC1	100 % Al-6061 + (0 % $\text{CeO}_2$ + 0 % GNPs)
2	HAIMNC2	96 % Al-6061 + (3 % $\text{CeO}_2$ + 1 % GNPs)
3	HAIMNC3	96 % Al-6061 + (1 % $\text{CeO}_2$ + 3 % GNPs)
4	HAIMNC4	94 % Al-6061 + (3 % $\text{CeO}_2$ + 3 % GNPs)

**Characterization techniques**

The developed HAIMNCs sub-surface was observed using field-emission scanning electron microscopy (FESEM). Examination of the fabricated HAIMNCs revealed the dispersion nature of the reinforcement in the matrix material. The mixture's experimental density was measured using Archimedes' rule and ASTM B 962-13. The mixing rule was utilized to compute theoretical density. The predicted and experimental densities were used to determine the mixture's porosity. The theoretical density of the hybrid composite can be derived as Eq. (1) [12]:

$$\rho_{HAIMNCs} = \rho_{Al-6061} W_{Al-6061} + \rho_{Graphene} W_{Graphene} + \rho_{Ceria} W_{Ceria}. \tag{1}$$

Relative densification (%) can be derived from Eq. (2) [13]:

$$Relative\ densification\ (\%) = \left( \frac{Experimental\ density}{Theoretical\ density} \times 100 \right). \tag{2}$$

The porosity (%) of the specimens was calculated using Eq. (3) [14]:

$$Porosity\ (\%) = \left( 1 - \frac{Relative\ densification}{100} \right). \tag{3}$$

Before putting the test specimens through the Vickers hardness tester, they were rigorously wiped and buffed. On each of the 10 places, a load of 200 g was applied for a period of 20 seconds during the dwell time, after which the average was taken and noted. The tensile and yield strengths were determined based on the Vickers hardness values in MPa by applying Cahoon's Eqs. 4 and 5, which were recommended and suggested by Cahoon et al. [15] and acknowledged by various researchers [16–18].

$$Tensile\ strength\ (MPa) = \frac{VHN}{2.9} \times \left( \frac{m}{0.217} \right)^m, \tag{4}$$

$$Yield\ strength\ (MPa) = \frac{VHN}{3} \times 0.1^m, \tag{5}$$

where *VHN* and *m* are the Vickers hardness (MPa) and the strain-hardening exponent, respectively. In this study, *m* was set to 0.02, which should be less than unity, as reported by Callister and Rethwisch [19].

**Results and Discussions**

**Physical properties.** Figure 2 shows a graphical representation of the theoretical and experimental densities of the HAIMNCs samples. The analysis showed the dense nature of the stir-cast HAIMNCs owing to their high theoretical densities compared to the experimental densities. To calculate the theoretical densities of different HAIMNCs samples, Equation (1) was used, and the values after calculations are as follows.

**Table 2.** Densities of HAIMNCs samples

Samples / Nomenclature	Theoretical densities, g/cm <sup>3</sup>	Experimental density, g/cm <sup>3</sup>
HAIMNC1	2.71	2.68
HAIMNC2	2.78	2.76
HAIMNC3	2.68	2.67
HAIMNC4	2.88	2.87

**Table 3.** Densification and porosities of HAIMNCs samples

Samples / Nomenclature	Relative densification, %	Porosity, %
HAIMNC1	98.89	1.11
HAIMNC2	99.05	0.95
HAIMNC3	99.32	0.68
HAIMNC4	99.42	0.58

A graphical representation of the physical properties, such as the experimental and theoretical densities in Table 2 and the densifications and porosities are presented in Table 3. The densities increased linearly with an increase in the nano-reinforcements, as shown in Fig. 2.

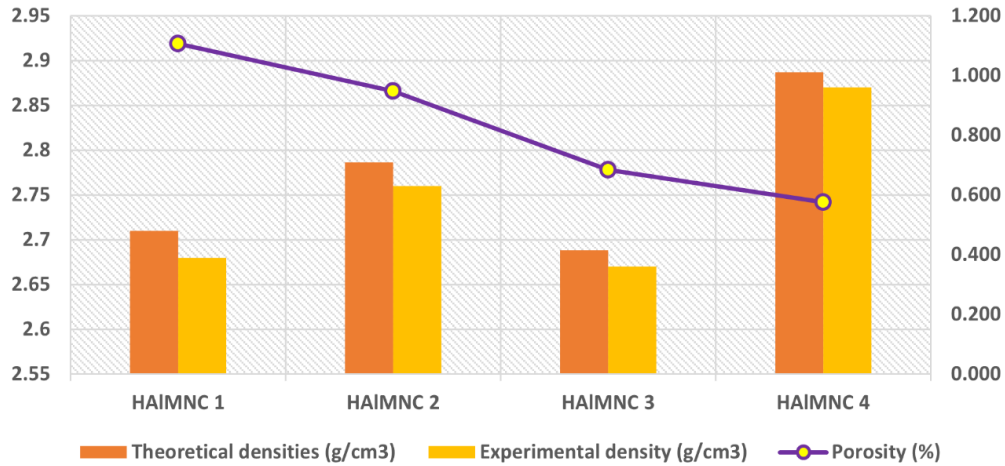


**Fig. 2.** Physical properties of stir-casted HAIMNCs samples

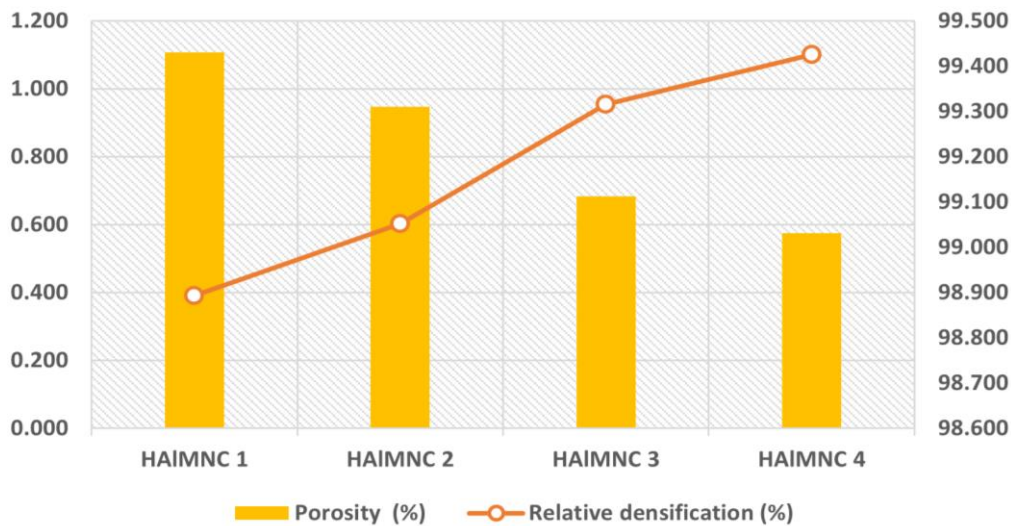


**Fig. 3.** Plot of relative densification vs density

Figure 3 illustrates relative densification (%) and porosity (%) of developed HAIMNCs samples. The theoretical data (Table 2) revealed certain decrement in porosity and increment in densification as nano-reinforcement wt. % increased. Both physical characteristics are inversely proportional in nature. The hybrid composite's relative densification increased when CeO<sub>2</sub> and GNP weight percentages increased. The uniform dispersion of both nano-reinforcements could be the reason for the decrease in the porosity. A decrease of 69.5 % in porosity was observed in HAIMNC4 sample compared to HAIMNC1. The effect on the porosity was observed with the addition of CeO<sub>2</sub> to Al6061-SiC-Al<sub>2</sub>O<sub>3</sub> using a stir-casting route. Furthermore, the porosity decreases with increasing CeO<sub>2</sub> content (0.5, 1.5, and 2.5 wt. %) in the hybrid composites [20]. MMCs made of A356-15 % ZrO<sub>2</sub> were produced by Abdizadeh et al. using a stir casting process at 750 °C. Within the same composition of the MMCs, an increase of 10 % in density and a hardness increase of 52 % were also found [21]. Leo et. al. prepared Al-8090/2 % SiC/x % B<sub>4</sub>C hybrid composites, where x = 2, 4, and 6 %, using the stir casting method. The results showed a decrease in density with the reinforcement percentage in the HMMCs. The 2.53 g/cm<sup>3</sup> actual density was observed in as-casted Al-8090 alloy and lowest density 2.51 g/cm<sup>3</sup> was found in Al-8090/6 % B<sub>4</sub>C/2 % SiC specimen [22]. Similarly, Tamuly et al. observed that an increase in the weight percentage increases the density of the fabricated

material owing to grain refinement after the fabrication of a cast aluminum composite [23]. Stir-cast AMCs strengthened with SiC and Mo were prepared by Kumar et al. The findings showed that the AMCs samples with a higher volume percentage of reinforcements had higher densities. [24]. The current study strictly followed the trends of previous studies, and the porosity values were within the acceptable range. The relative densification (ratio of theoretical to experimental density) increased with increasing reinforcement wt. %. This can be attributed to an enhancement in the wettability of the HAIMNCs as the reinforcement weight percentage increased in the matrix material, which was the result of proper dispersion of the reinforcement particles in the base alloy [25].

**Mechanical properties.** The microhardness, tensile strength, and yield strength of the test specimens are presented in Fig. 4. An increase of 53.85 % (from 53 to 80 VHN) was recorded when Al-6061 was reinforced with 3GNPs and 1CeO<sub>2</sub>. Further, 86.35 and 100.58 % increment was observed as compared to base alloy with addition of (3CeO<sub>2</sub> + 1 GNPs) and (3GNPs + 3CeO<sub>2</sub>) wt. % reinforcement to matrix material. An enrichment in hardness values was observed with reference to previous findings. Prakash et al. stirred a composite of Al-6061 alloy reinforced with multi-walled CNTs with various wt. %. The increment of 18.6, 11.93, and 66.6 % in hardness, tensile, and impact strength, respectively, in the MMCs by 1.5 wt. % addition of MWCNTs. The proper distribution of MWCNTs particles in the Al-6061 alloy matrix was also determined through microstructural investigation [26]. Vipin Kumar Sharma et al. [27] observed the effect of cerium oxide (CeO<sub>2</sub>) on hybrid composites. The 2.5 wt. % of CeO<sub>2</sub> gives the optimum values for mechanical properties like; hardness increased by 17.02 %, tensile strength increased with 80 and 78 % increment gain in flexural strength of fabricated hybrid composite. The wear behavior was also observed to enhanced by 87.28 % with the same composition in fabricated hybrid composite [27]. Table 5 presents the theoretical mechanical properties of the fabricated HAIMNCs samples.

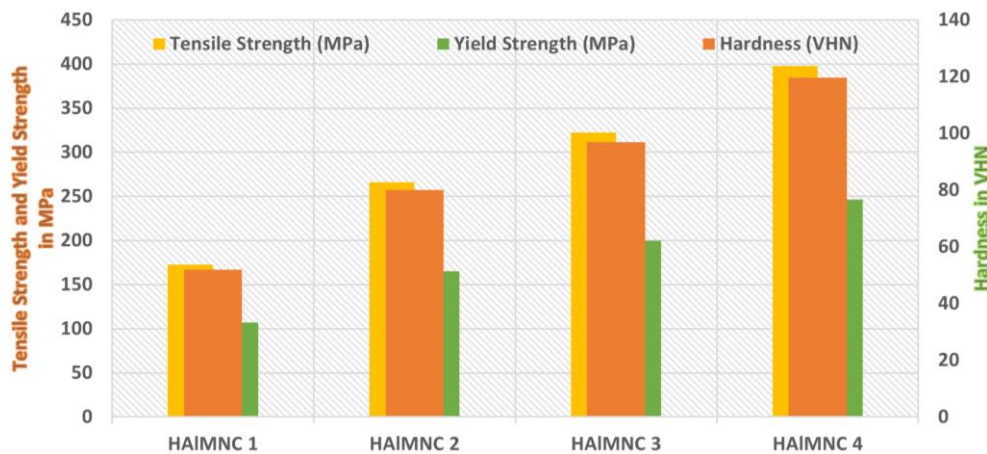


**Fig. 4.** Theoretical mechanical properties of HAIMNCs samples

**Table 5.** Mechanical properties of HAIMNCs samples

Sample Number	Hardness, VHN	Tensile Strength, MPa	Yield Strength, MPa
HAIMNC1	52.00	173.00	107.26
HAIMNC2	80.00	266.16	165.01
HAIMNC3	96.90	322.39	199.87
HAIMNC4	119.60	397.90	246.68

The highest tensile strength (347.01 MPa in the HAIMNC4 specimen. The HAIMNC1 specimen exhibited the lowest tensile strength (173 MPa). The contribution of various stir-casting parameters enhanced the tensile strength. Senthil Kumar et al. [28] cast A356 alloy/6 % TiB<sub>2</sub>

MMCs at various temperatures. Three levels of pouring temperature were chosen: 750, 780, and 810 °C. The effect on hardness was observed at these pouring temperatures. It has been noted that hardness increases linearly with increasing pouring temperature [28].

Shayan et al. [29] examined the effects of TiO<sub>2</sub> as a reinforcement particle in a molten matrix AA2024. According to the research conducted, ductility in terms of elongation increased by 163 % and hardness increased by 25 % compared to base alloys. A 28 % increase was observed in ultimate tensile strength, and 4 % growth was seen in modulus of elasticity when compared to matrix alloys [29]. Gireesh et al. [30] fabricated the stir-cast HAMMC reinforced with SiC and Al<sub>2</sub>O<sub>3</sub> particulates at a constant weight fraction (5 %). The aim of this study was to improve the hardness and strength of the fabricated Al-6061/SiC/ Al<sub>2</sub>O<sub>3</sub> HAMMCs. A 10 % increase was observed in hardness, 15 % improvement in terms of tensile strength, and 6 % growth was seen in yield strength of the produced HAMMCs [30]. Amouri et al. [31] also reported that the tensile and compressive strengths were enhanced in a composite material with 1.5 wt. % of nano SiC particles to the A356 aluminum alloy fabricated through stir casting method. The tensile strength of 232 MPa was achieved with stir-cast MMCs of A356-15 % ZrO<sub>2</sub> composites produced at 750 °C. An increment of 10 and 52 % in density and hardness was also observed for the same composition of the MMCs [21]. HAIMNC4 specimen exhibited a maximum yield strength of 215.13 MPa, which was 100.57 % that of Al-6061 alloy (107.26 MPa). The present study attributes uniform dispersion to the enhancement of mechanical characteristics.

**Microstructure analysis.** SEM and EDAX micrographs of the stir-cast HAIMNCs samples are shown in Fig. 5. Four regions were observed in the SEM images: Grey represented the Al-6061 alloy, white represented CeO<sub>2</sub>, and black represented GNPs in the SEM images, respectively. Finally, the porosity of the HAIMNCs sample is represented by darker shades of grey.

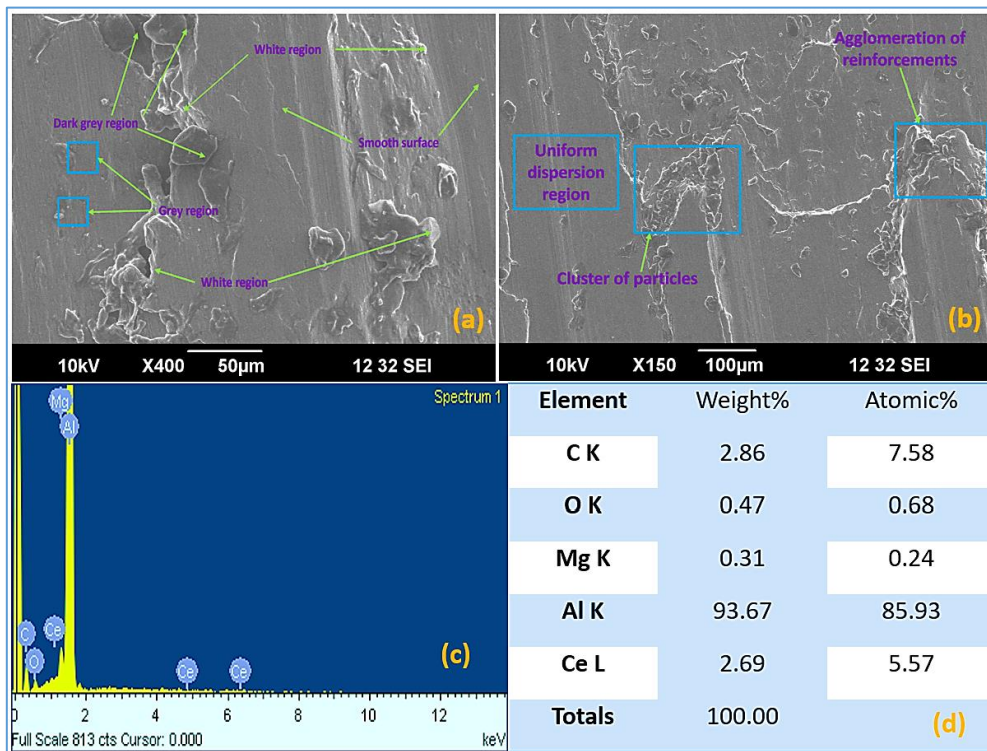


**Fig. 5.** Specimens SEM Images: (a) HAIMNC2; (b) HAIMNC4; (c) HAIMNC4 EDAX spectrum, and (d) HAIMNC4 EDAX with element wt. %

A change in the microstructural behavior was observed owing to the addition of the nano-reinforcements. A uniform dispersion and defect-free morphology can be observed in the HAIMNCs specimens compared with the base material. EDAX analysis verified the incorporation of nano reinforcement particles into the hybrid composite with the inclusion of

Mg for enhanced wettability. Hexa-chloro-ethane tablets were also used to avoid the harmful reactions observed in the HAIMNCs specimens. Strong contact between the matrix material and reinforcements improves the mechanical characteristics of the manufactured composites, as was also observed in previous investigations. Anandaraj et al. [32] utilized a liquid metallurgical method to create AA5083-MoO<sub>3</sub> composites and investigated their characteristics. Molybdenum trioxide (MoO<sub>3</sub>) has been investigated as a reinforcement to improve the performance of metal-matrix composites (MMCs). Composites were prepared by incorporating varying amounts of MoO<sub>3</sub> into an AA5083 matrix. In this study, we compare AA5083 to AA5083 with 4 wt. % MoO<sub>3</sub>, AA5083 with 8 wt. % MoO<sub>3</sub>, and AA5083 with 12 wt. % MoO<sub>3</sub>. Composites with 12 wt. % MoO<sub>3</sub> had the highest tensile strength (207 MPa) [32]. Raja et al. [33] produced hybrid aluminum surface composites. Reinforcing particles consisting of boron carbide (B<sub>4</sub>C), silicon carbide (SiC), and calcium carbonate (CaCO<sub>3</sub>) were combined at a 1:1:1 ratio to create a hybrid mixture. The fabrication procedure involved three different hybrid reinforcement weight percentages: 5 (T1), 10 (T2), and 15 % (T3). Sample T3, with 15 % reinforcement content, outperformed samples T1 and T2 in Ultimate Tensile strength (UTS) by 62.63 and 15.17 percent, respectively. However, when comparing these samples, T3's Elongation (%) was lower by 38.46 (T1 sample) and 15.38 % (T1 sample), respectively. Sample T3 exhibited a more brittle reaction, as evidenced by its higher hardness in the stirred zone compared to the other two samples. The microstructural investigation verified the presence of reinforcements and their distribution in the stir zone [33]. In keeping with these developments, the current study demonstrates that including GNPs and CeO<sub>2</sub> in the melting process enhances the metal fluidity and, in turn, the mechanical properties of the resulting HAIMNCs. The porosity of the manufactured HAIMNCs samples was shown to increase inversely with their reinforcement content, as validated by scanning electron microscopy [34–36].

## Conclusions

The physical, mechanical, and microstructural characteristics of the fabricated nanocomposite were examined, and the following conclusions were drawn.

1. An aluminum nanocomposite was successfully fabricated and reinforced by the addition of GNPs and CeO<sub>2</sub> nanoparticles using a stir-casting route.
2. A hybrid aluminum composite containing GNPs and CeO<sub>2</sub> nanoparticles (1–3 wt. %) possesses improved physical and mechanical properties compared to as-casted sample.
3. The experimental and theoretical densities increased with the addition of the reinforcement percentages, and the porosity decreased for identical percentages of GNPs and CeO<sub>2</sub>. The density and porosity were inversely proportional to each other.
4. Vickers hardness, tensile strength, and yield strength were all maximised at 104.3, 352.01, and 207.98 MPa, respectively, when reinforcing nanoparticles proportions of 3 % CeO<sub>2</sub> and 3 % GNPs were added to Al-6061 alloy.
5. The microstructural study confirmed the uniform dispersion and defect-free morphology of the hybrid aluminum nanocomposite specimens. No cracks or pores are observed in the fabricated nanocomposites. This is because of the refined grain size and the bonding action of the reinforcements in the HAIMNCs sample with 3 % GNPs and 3 % CeO<sub>2</sub> proportions.

## References

1. Kumar D, Angra S, Singh S. Mechanical Properties and Wear Behaviour of Stir Cast Aluminum Metal Matrix Composite: A Review. *Int. J. Eng. Trans. A Basics*. 2022;35: 794–801.
2. Yeshiye T, Gizaw M. A review on Effects of reinforcements on properties and wear



- behaviour of aluminium metal matrix material. *International Journal of Renewable Energy Technology*. 2021;6: 1–17.
3. Kumar D, Singh S, Angra S. Dry sliding wear and microstructural behavior of stir-cast Al6061-based composite reinforced with cerium oxide and graphene nanoplatelets. *Wear*. 2023;516–517: 204615.
  4. Kumar D, Angra S, Singh S. High-temperature dry sliding wear behavior of hybrid aluminum composite reinforced with ceria and graphene nanoparticles. *Eng. Fail. Anal.* 2023;151: 107426.
  5. Kumar D, Singh S, Angra S. Morphology and Corrosion Behavior of Stir-Cast Al6061- CeO<sub>2</sub> Nanocomposite Immersed in NaCl and H<sub>2</sub>SO<sub>4</sub> Solutions. *Evergr. Jt. J. Nov. Carbon. Resour. Sci. Green. Asia Strateg.* 2023;10: 94–104.
  6. Aktaş S, Anıl Diler E. Effect of ZrO<sub>2</sub> Nanoparticles and Mechanical Milling on Microstructure and Mechanical Properties of Al-ZrO<sub>2</sub> Nanocomposites. *J. Eng. Mater. Technol.* 2021;143: 041002.
  7. Nojima A, Sano A, Kitamura H, Okada S. Electrochemical Characterization, Structural Evolution, and Thermal Stability of LiVOPO<sub>4</sub> over Multiple Lithium Intercalations. *Evergr. Jt. J. Nov. Carbon Resour. Sci. Green Asia Strateg.* 2019;6: 267–274.
  8. Aydin F, Turan ME. The Effect of Boron Nitride on Tribological Behavior of Mg Matrix Composite at Room and Elevated Temperatures. *J. Tribol.* 2020;142: 011601.
  9. Hugar N, Prashanth S, Lalji P, Hegde SG, Narayana BV, Kumar KM, Waddar S. Fabrication and characterization of high performance aluminium composites for automotive components. *AIP Conf. Proc.* 2022;2421: 040006.
  10. Li T, Davies JMT, Zhu X. Effect of carrier gases on the entrainment defects within AZ91 alloy castings. *J. Magnes. Alloy.* 2022;10: 129–145.
  11. Murugan S, Jegan S, Velmurugan V. Tribological Wear Behaviour and Hardness Measurement of SiC, Al<sub>2</sub>O<sub>3</sub> Reinforced Al Matrix Hybrid Composite. *J. Inst. Eng. Ser. D.* 2017;98: 291–296.
  12. Krishan K, Chawla. *Composite Materials: Science and Engineering*. 2019.
  13. Rm SS, Ramanathan K. A study on tribological behaviour and analysis of ZnO reinforced AA6061 matrix composites fabricated by stir casting route. *Industrial Lubrication and Tribology*. 2021;4: 642–651.
  14. Zhang WY, Du YH, Zhang P. Vortex-free stir casting of Al-1.5 wt% Si-SiC composite. *J. Alloys Compd.* 2019;787: 206–215.
  15. Cahoon JR. *The Determination of Yield Strength From Hardness Measurements*. 1979.
  16. Ujah C, Popoola P, Popoola O, Aigbodion V. Enhanced mechanical, electrical and corrosion characteristics of Al-CNTs-Nb composite processed via spark plasma sintering for conductor core. *Journal of Composite Materials*. 2019;53(26-27): 3775–3786.
  17. Annaz AA, Irhayyim SS, Hamada ML, Hammood HS. Comparative study of mechanical performance between Al – Graphite and Cu – Graphite self-lubricating composites reinforced by nano-Ag particles. *AIMS Materials Science*. 2020;7(5): 534–551.
  18. Irhayyim SS, Hammood HS, Abdulhadi HA. Effect of nano-TiO<sub>2</sub> particles on mechanical performance of Al – CNT matrix composite. *AIMS Materials Science*. 2019;6(6): 1124–1134.
  19. Callister WD, Rethwisch DG. *Materials Science and Engineering. An Introduction*. John Wiley & Sons, Inc.; 2018.
  20. Kumar V, Kumar V, Singh R. Parametric study of aluminium-rare earth based composites with improved hydrophobicity using response surface method. *Integr. Med. Res.* 2020;9: 4919–4932.
  21. Abdizadeh H, Baghchesara MA. Investigation into the mechanical properties and fracture behavior of A356 aluminum alloy-based ZrO<sub>2</sub>-particle-reinforced metal-matrix composites. *Mech. Compos. Mater.* 2013;49: 571–576.
  22. Leo Bright Singh R, Jinu GR, Manoj M, Elaya Perumal A. Tribological Behaviour of Al8090-

- SiC Metal Matrix Composites with Dissimilar B<sub>4</sub>C Addition. *Silicon*. 2022;14: 8895–8908.
23. Tamuly R, Behl A, Borkar H. Effect of Addition of Grain Refiner and Modifier on Microstructural and Mechanical Properties of Squeeze Cast A356 Alloy. *Trans. Indian Inst. Met.* 2022;75: 2395–2408.
24. Kumar J, Singh D, Kalsi NS, Sharma S, Mia M, Singh J, et al. Investigation on the mechanical, tribological, morphological and machinability behavior of stir-casted Al/SiC/Mo reinforced MMCs. *J. Mater. Res. Technol.* 2021;12: 930–946.
25. Kumar D, Singh PK. ScienceDirect Microstructural and Mechanical Characterization of Al-4032 based Metal Matrix Composites. *Mater. Today Proc.* 2019;18: 2563–2572.
26. Prakash B, Sivananthan S, Vijayan V. Materials Today : Proceedings Investigation on mechanical properties of Al6061 alloy – Multiwall carbon nanotubes reinforced composites by powder metallurgy route. *Mater. Today Proc.* 2020;37: 336–340.
27. Sharma VK, Kumar V, Joshi RS. Investigation of rare earth particulate on tribological and mechanical properties of Al-6061 alloy composites for aerospace application. *Integr. Med. Res.* 2019;8: 3504–3516.
28. Senthil Kumar P, Kavimani V, Soorya Prakash K, Murali Krishna V, Shanthos Kumar G. Effect of TiB<sub>2</sub> on the Corrosion Resistance Behavior of In Situ Al Composites. *Int. J. Met.* 2020;14: 84–91.
29. Shayan M, Eghbali B, Niroumand B. Fabrication of AA2024–TiO<sub>2</sub> nanocomposites through stir casting process. *Trans Nonferrous Met Soc China*. 2020;30: 2891–2903.
30. Gireesh CH. Experimental Investigation on Mechanical Properties of an Al6061 Hybrid Metal Matrix Composite. *J. Compos. Sci.* 2018;2(3): 49.
31. Amouri K, Kazemi S, Momeni A, Kazazi M. Microstructure and mechanical properties of Al-nano/micro SiC composites produced by stir casting technique. *Mater. Sci Eng. A*. 2016;674: 569–578.
32. Anandaraj T, Sethusundaram PP, Meignanamoorthy M, Ravichandran M. Investigations on properties and tribological behavior of Investigations on properties and tribological behavior of method. *Surf. Topogr.: Metrol. Prop.* 2021;9(2): 025011.
33. Raja R, Shanmugam R, Jannet S, Kumar GBV, Venkateshwaran N, Naresh K, Ramoni M. Development of Al-Mg<sub>2</sub>Si Alloy Hybrid Surface Composites by Friction Stir Processing: Mechanical, Wear, and Microstructure Evaluation. *Materials*. 2023;16(11): 4131.
34. Hima Gireesh C, Durga Prasad K, Ramji K. Experimental Investigation on Mechanical Properties of an Al6061 Hybrid Metal Matrix Composite. *J. Compos. Sci.* 2018;2: 49.
35. Ponugoti GR, Alluru GK, Vundavilli PR. Response Surface Methodology Based Modelling of Friction–Wear Behaviour of Al6061/9%Gr/WC MMCs and Its Optimization Using Fuzzy GRA. *Trans. Indian Inst. Met.* 2018;71: 2465–2478.
36. Królczyk G, Feldshtein E, Dyachkova L, Michalski M, Baranowski T, Chudy R. On the microstructure, strength, fracture, and tribological properties of iron-based MMCs with addition of mixed carbide nanoparticulates. *Materials*. 2020;13(13): 2892.

## THE AUTHORS

**Kumar Dinesh** 

e-mail: dinesh\_61900120@nitkkr.ac.in

**Singh Satnam** 

e-mail: satnamsingh@nitkkr.ac.in

**Angra Surjit**

e-mail: surjit.angra@yahoo.com